Korean J Physiol Pharmacol 2018;22(3):321-329
https://doi.org/10.4196/kjpp.2018.22.3.321

KJPP

Original Article

Physiologically-based pharmacokinetic predictions of intestinal BCRP-mediated drug interactions of rosuvastatin in Koreans

Soo Hyeon Bae[1,2], Wan-Su Park[1,2], Seunghoon Han[1,2], Gab-jin Park[1,2], Jongtae Lee[1,2], Taegon Hong[3], Sangil Jeon[4], and Dong-Seok Yim[1,2,*]

[1]Department of Clinical Pharmacology and Therapeutics, Seoul St. Mary's Hospital, Seoul 06591, [2]PIPET (Pharmacometrics Institute for Practical Education and Training), College of Medicine, The Catholic University of Korea, Seoul 06591, [3]Department of Clinical Pharmacology, Severance Hospital, Yonsei University College of Medicine, Seoul 03722, [4]Q-fitter Inc., Seoul 06199, Korea

ARTICLE INFO

Received November 16, 2017
Revised January 17, 2018
Accepted February 19, 2018

***Correspondence**
Dong-Seok Yim
E-mail: yimds@catholic.ac.kr

Key Words
Cyclosporine
Intestinal BCRP transporter
Physiologically-based pharmacokinetics
Rosuvastatin
Telmisartan

ABSTRACT It was recently reported that the C_{max} and AUC of rosuvastatin increases when it is coadministered with telmisartan and cyclosporine. Rosuvastatin is known to be a substrate of OATP1B1, OATP1B3, NTCP, and BCRP transporters. The aim of this study was to explore the mechanism of the interactions between rosuvastatin and two perpetrators, telmisartan and cyclosporine. Published (cyclosporine) or newly developed (telmisartan) PBPK models were used to this end. The rosuvastatin model in Simcyp (version 15)'s drug library was modified to reflect racial differences in rosuvastatin exposure. In the telmisartan–rosuvastatin case, simulated rosuvastatin C_{maxI}/C_{max} and AUC_I/AUC (with/without telmisartan) ratios were 1.92 and 1.14, respectively, and the T_{max} changed from 3.35 h to 1.40 h with coadministration of telmisartan, which were consistent with the aforementioned report (C_{maxI}/C_{max}: 2.01, AUC_I/AUC:1.18, T_{max}: 5 h → 0.75 h). In the next case of cyclosporine–rosuvastatin, the simulated rosuvastatin C_{maxI}/C_{max} and AUC_I/AUC (with/without cyclosporine) ratios were 3.29 and 1.30, respectively. The decrease in the $CL_{int,BCRP,\ intestine}$ of rosuvastatin by telmisartan and cyclosporine in the PBPK model was pivotal to reproducing this finding in Simcyp. Our PBPK model demonstrated that the major causes of increase in rosuvastatin exposure are mediated by intestinal BCRP (rosuvastatin–telmisartan interaction) or by both of BCRP and OATP1B1/3 (rosuvastatin–cyclosporine interaction).

INTRODUCTION

It is known that about one-third of deaths worldwide (i.e., ~17.3 million per year) are caused by cardiovascular dysfunctions [1]. Among patients with cardiovascular disease, 30.7% of patients were found to have both hypertension and dyslipidemia, and 66.3% of patients with diabetes had concomitant hypertension and dyslipidemia, in a 3-year retrospective study [2]. Thus, multiple drug therapy has been widely practiced for the treatment of problems including hypertension and dyslipidemia. Rosuvastatin, a 3-hydroxy-3-methylglutaryl-coenzyme A (HMG-CoA) reductase inhibitor, is commonly used in combination with telmisartan, an angiotensin II type-I receptor antagonist (ARB). Recently, Son et al. [3] reported increased pharmacokinetic (PK) exposure of rosuvastatin when coadministered with telmisartan. The absorption of rosuvastatin was accelerated (C_{max} was doubled, with T_{max} change from 5 h to 0.75 h.), whereas its AUC increased by only 1.18-fold when coadministered with telmisartan, although the cause of this phenomenon was not identified by the authors. In addition to the rosuvastatin–telmisartan interaction, it is well-known that cyclosporine also increases rosuvastatin AUC and C_{max} by 1.5- and 3.0-fold and more severe interaction was

Author contributions: S.H.B. and W.P. conducted PBPK modeling of rosuvastatin and telmisartan and drafted the manuscript. S.H., G.P., J.L., T.H., and S.J. contributed to clinical data generation and D.S.Y. finalized the manuscript and supervised the study.

reported in transplant recipients (>6 months, stable heart transplant recipients): the AUC and C_{max} ratios of rosuvastatin (with/without cyclosporine) were of 7.1- and 10.6-fold, respectively [4,5]. Cyclosporine is an inhibitor of many transporters including OATP1B1/1B3, NTCP, and BCRP transporters and the rosuvastatin–cyclosporine interaction is known to be mediated by transporters.

Telmisartan prevents angiotensin II from exerting its vasoconstrictive effects on blood vessels, and thus has been widely used for the treatment of hypertension [6,7]. It has been reported that telmisartan is rapidly absorbed in the gastrointestinal tract (T_{max} 0.75 h) [3] and is predominantly transported into the liver by organic anion transporting polypeptide (OATP) 1B3 [7], to be metabolized to an acylglucuronide conjugate by hepatic UDP-glucuronosyltransferase (UGT) 1A3 [8], such that no unchanged parent molecule is excreted [9]. Recently, Hirano et al. [10] reported that telmisartan potently inhibited OATP1B1-mediated pravastatin uptake (inhibitory constant (K_i), 0.436 μM) and OATP1B3-mediated dioscin uptake (K_i, 1.03 μM) *in vitro* [11]. In addition to uptake transporter inhibition, telmisartan is also known to be a non-specific inhibitor of ATP-binding cassette (ABC) transporters, such as P-glycoprotein (P-gp), breast cancer resistance protein (BCRP) [12], and multidrug resistance-associated protein 2 (MPR2) [13].

Rosuvastatin, a highly selective and competitive HMG-CoA reductase inhibitor, reduces LDL and increases HDL cholesterol levels in blood [14]. It is mainly excreted unchanged into bile [15,16], and less than 10% is metabolized to *N*-desmethylrosuvastatin by CYP2C9 [17]. Rosuvastatin is extensively distributed into the liver, presumably due to active uptake by OATP1B1 and OATP1B3, as well as by the sodium-dependent taurocholated co-transporting polypeptide (NTCP) transporters [18-20], despite its low passive diffusion into hepatocytes [4,15,21]. It is also a substrate of both liver canalicular and intestinal BCRP efflux transporters [21-23].

Nowadays, it has been reported that the increased rosuvastatin exposure by concomitant medication is mediated by the BCRP transporter, rather than by OATP1B1/1B3 transporters [24,25]. The aim of this study is to explore the mechanism of the transport-mediated interaction between rosuvastatin and two perpetrators, telmisartan and cyclosporine. Although many researchers have reported that PK changes of rosuvastatin are mainly due to OATP1B1-mediated interactions, we demonstrate here that alterations in the PK of rosuvastatin upon coadministration with telmisartan are mainly mediated by their sharing BCRP, not OATP1B1/1B3, transporters, using a physiologically based PK (PBPK) model. We also describe rosuvastatin and cyclosporine DDI with PBPK model focusing on transporter-mediated interactions. Moreover, because Asians show higher systemic exposure of rosuvastatin than Caucasians do [26,27], the PBPK model reflecting exposures in Koreans was applied to the rosuvastatin model. PBPK modeling provides a bottom-up approach to PK predictions with integration of diverse information on human physiology, physiochemical properties of drugs, and drug metabolizing enzymes and transporters. Simcyp (version 15 release 1, Certara, Sheffied, UK) was used in this report to explore the contributions of BCRP and OATP1B1/1B3 transporters to drug interactions and to predict the PK of rosuvastatin.

A part of this paper was presented at the 11th international ISSX meeting (2016). A part of this study was first published as an original article in Biopharm Drug Dispos 2017; doi: 10.1002/bdd.2060, but was retracted by the authors because trivial miscalculations incurred by one misused input parameter were found throughout the simulated values in the article. For further details, please read doi: 10.1002/bdd.2082.

METHODS

Development of the telmisartan model

Simcyp (version 15 release 1, Certara, Sheffield, UK) was used to simulate and predict the time course of rosuvastatin in plasma with or without telmisartan. The telmisartan model was developed based on the report by Li et al. [28], where many of the physiochemical properties and *in vitro* PK parameters of telmisartan used herein are listed in Table 1. The simulation of telmisartan plasma concentration–time profiles was performed using a full-PBPK model of first-order absorption. The k_a and F_a values are from Li et al. [28], and the nominal flow in gut model (Q_{gut}), which reflects both permeability through the enterocyte membrane and villous blood flow [29], was estimated by Simcyp to be 15.564 L/h based on telmisartan physiochemical properties. The human PET data-derived k_p values [28] for adipose tissue, bone, brain, gut, heart, kidney, lung, muscle, skin, and spleen used in this study were 0.35, 0.47, 0.25, 1.67, 1.54, 4.4, 1.07, 0.40, 0.26, and 0.41, respectively. However, we used the value reported by Rodgers and Rowland (0.12) [28,30] for the hepatic k_p because PET cannot discern telmisartan in hepatocytes from its metabolite, telmisartan-glucuronide, whose concentration is much higher than that of the parent compound in the liver [28]. The steady-state volume of distribution (V_{ss}) was then estimated as 0.41 L/kg based on the aforementioned k_p values using mathematical model 2 implemented in Simcyp [28]. For the telmisartan CL_{po}, the mean value reported in healthy subjects (25.2 L/h) was used [3].

Before the evaluation of telmisartan–rosuvastatin pharmacokinetic interactions, a clinical trial simulation of telmisartan was performed with virtual healthy populations (aged 20-50, female ratio of 0.5) in 10 trials of 10 subjects each. Simulated PK parameters and concentration–time profiles of telmisartan after a single and multiple (80 mg) oral administration were compared with observed PK data for validation.

Table 1. Physiochemical and pharmacokinetic parameters of telmisartan and cyclosporine used in PBPK modeling

Parameters (unit)	Telmisartan	Reference	Cyclosporine[a]
Molecular weight (g/mol)	514.62		1,202
$logD_{7.4}$	2.5	[28]	2.96 (logP)
pK_a	3.8	[28]	
Compound type	Monoprotic Acid	[28]	Neutral
B/P ratio	0.78	[9]	1.36
$f_{u,plasma}$	0.005	[9]	0.0365
$f_{u,liver}$	0.013	[28]	
$f_{u,gut}$	0.015	Predicted by Simcyp	
F_a	0.72	[28]	0.857
k_a (h^{-1})	0.68	[28]	0.679
CL_{po} (L/h)	25.2	[3]	24.07 (CL_{iv})
$K_{i,OATP1B1,\ hepatic}$ (μM)	0.436	[10]	0.014
$K_{i,OATP1B3,\ hepatic}$ (μM)	1.03	[11]	0.007
$K_{i,BCRP}$ (μM)	0.005	Estimated by Parameter Estimation	0.28

[a]All data are from [4].

Modification of the rosuvastatin model

A PBPK model of rosuvastatin in a European Caucasian healthy volunteer population was previously constructed in Simcyp's drug library. Because Asians show higher systemic exposure of rosuvastatin than do Caucasians [26], the recommended starting dose for Asians (5 mg) is lower than that for Caucasians (10 mg) [27]. Although the cause of these racial differences is unclear, one possible explanation is that there may be differences in the activity or expression levels of uptake transporters of rosuvastatin, such as OATP1B1, OATP1B3, and NTCP, and/or an efflux transporter, such as BCRP. Because the PK data of a telmisartan–rosuvastatin interaction study conducted in Korean healthy volunteers were used as the reference [3], the rosuvastatin model in Simcyp's drug library was modified to reflect PK profiles in Koreans. Using Sensitivity Analysis (SA) and Parameter Estimation (PE) modules, the hepatic uptake clearance values of OATP1B1, OATP1B3, and NTCP for rosuvastatin were modified step-by-step to recover the published mean plasma concentration-time profile of rosuvastatin in Korean populations [3,31,32] from 5 different studies, whose data were obtained by digitization (Plot Digitizer, version 2.6.6, http://plotdigitizer.sourceforge.net). After these modifications, rosuvastatin concentrations in 10 virtual trials (10 healthy subjects per trial, aged 20-50, male/female=1:1) after a single (20 mg) oral dose were simulated in Simcyp.

Evaluation of the effects of telmisartan on the PK of rosuvastatin using PBPK modeling

Estimation of $K_{i,BCRP,intestine}$ of telmisartan: Based on the above telmisartan and rosuvastatin models, telmisartan–rosuvastatin interaction was predicted. The *in vitro* inhibitory constants of telmisartan against hepatic OATP1B1 ($K_{i,OATP1B1,hepatic}$) and OATP1B3 ($K_{i,OATP1B3,hepatic}$) have been reported as 0.436 μM and 1.03 μM, respectively [10,11]. Because there was no published K_i value of telmisartan against the intestinal BCRP transporter ($K_{i,BCRP,intestine}$), several methods were used to estimate the proper $K_{i,BCRP,intestine}$ value of telmasartan; 1) its half-maximal inhibitory concentration ($IC_{50,BCRP}$) [13] was used to calculate $K_{i,BCRP,intestine}$, by Eq. (1) described in [33]:

$$K_i=IC_{50}/(1+S/K_m) \quad (1)$$

where S is substrate concentration and K_m represents the Michaelis–Menten constant of the substrate. If S is near K_m values, then $K_{i,BCRP,intestine}$ would be $IC_{50}/2$. 2) In addition to using the estimated $K_{i,BCRP,intestine}$ value as $IC_{50}/2$, a sensitivity analysis (SA) comparing simulated and observed C_{max} and AUC ratios at varying $K_{i,BCRP,intestine}$ estimates was conducted. 3) Based on the $K_{i,BCRP,intestine}$ estimate obtained from SA, the parameter estimation (PE) module was used for the estimation of the $K_{i,BCRP,intestine}$ value.

Simulation of clinical study: Clinical trials in 100 virtual healthy subjects (10 trials×10 subjects per trial, aged 20-50, male:female=1:1) were simulated in Simcyp with a dosing scheme identical to that reported by Son et al. [3]. After rosuvastatin (20 mg qd) was given alone or together with telmisartan (80 mg qd) for six days, plasma concentration profiles of rosuvastatin were simulated to compare with those reported elsewhere [3,32] (Table 2). The profiles of rosuvastatin in the gut and liver were also predicted to elucidate the mechanisms of interaction.

Evaluation of the effects of cyclosporine on the PK of rosuvastatin using PBPK modeling

The cyclosporine model reported by Jamei et al. [4] was used (Table 1). We validated the model using the data digitized from two different human studies [34,35] (Plot Digitizer, version 2.6.6, http://plotdigitizer.sourceforge.net). Clinical trials in 100 vir-

Table 2. Observed and simulated (PBPK modeling) rosuvastatin pharmacokinetic (20 mg, multiple doses) exposures

Rosuvastatin exposure parameters		C_{max} (ng/mL)	AUC (ng h/mL)	T_{max} (h)[a]	C_{maxI}/C_{max}	AUC_I/AUC
Observed[b]	Without perpetrators	27.8	229	5.00		
	With telmisartan	56.0	270	0.75	2.01	1.18
Predicted[c]	Without perpetrators	24.4 (22.5-26.5)	226.0 (208.3-245.1)	3.35		
	With telmisartan	46.9 (42.6-49.8)	257.6 (238.6-277.3)	1.40	1.92	1.14
	With cyclosporine	80.3 (74.4-86.6)	293.4 (271.5-317.1)	1.00	3.29	1.30

[a]T_{max}'s are expressed as medians.
[b]Son et al., 2014 [3]; C_{max} and AUC are expressed as geometric means.
[c]C_{max} and AUC are expressed as geometric mean (95% prediction interval).

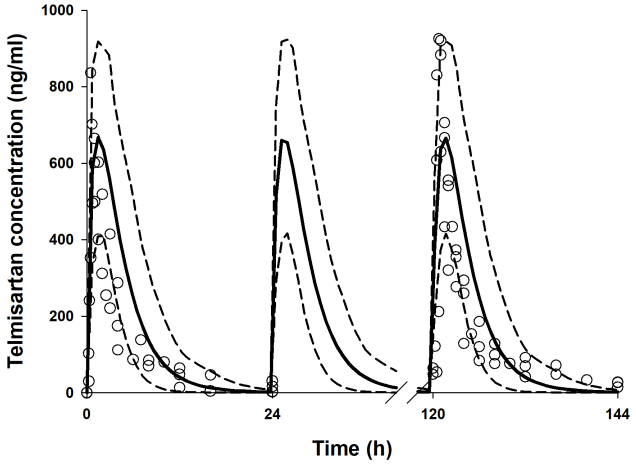

Fig. 1. Simulated and observed plasma telmisartan concentration–time profiles after a single and multiple (for 6 days) oral administration of 80 mg telmisartan. Solid line and dashed lines represent mean and 95th and 5th percentiles of simulated telmisartan concentrations and dots are observed data from references [8,36,37] for a single and [3,38,39] for multiple dosing, respectively.

tual healthy subjects (10 trials×10 subjects per trial, aged 20-50, male:female=1:1) were simulated for the evaluation of the effects of cyclosporine on rosuvastatin PK. The profiles of rosuvastatin (20 mg) PK were simulated with or without cyclosporine (200 mg, BID).

RESULTS

Development of the telmisartan model

Telmisartan plasma concentration–time profiles after single oral administration (80 mg) were simulated using its physicochemical parameters and PK parameters (Table 1). The C_{max}, AUC, and T_{max} after administration of telmisartan 80 mg predicted by Simcyp (10 trials of 10 subjects each) were similar to the published data [6,36,37] and the simulation results of multiple administrations of telmisartan 80 mg for 6 days also well explained the observed data (Fig. 1) [3,38,39].

Table 3. The summary of hepatic uptake clearances of rosuvastatin modified using clinical data in Koreans

Parameters (μl/min/10^6 cells)	In Simcyp drug's library (Caucasian)	After modification with clinical data
$CL_{int,hepatic,NTCP}$	78	19.7
$CL_{int,hepatic,OATP1B1}$	109	25.1
$CL_{int,hepatic,OATP1B3}$	36	7.5

Modification of the rosuvastatin model

The rosuvastatin model in the Simcyp drug library was modified by the authors to reproduce the C_{max} and AUC in Koreans, which are about twice as high as in Caucasians [19,40]. The total $CL_{int,\ uptake\ transporters}$ value estimated using the SA method was adjusted for the ratio of $CL_{int,hepatic,NTCP}$, $CL_{int,hepatic,OATP1B1}$, and $CL_{int,hepatic,OATP1B3}$ in Caucasians in Simcyp. The final CL_{int} values were determined by the PE method using observed data from 5 different studies in Koreans. Upon comparing the PK data reported from Koreans [3,31,32] with our Simcyp-simulated ones, the CL_{int} values of the hepatic uptake transporters of rosuvastatin were adjusted (Table 3): they were about 1/5 of CL_{int}s of European Caucasians (Pre-existing $CL_{int,hepatic,NTCP}$, $CL_{int,hepatic,OATP1B1}$, and $CL_{int,hepatic,OATP1B3}$ values of 78, 109, and 36 μl/min/10^6 cells in Simcyp were modified as 19.7, 25.1, and 7.5 μl/min/10^6 cells, respectively, to be used for our simulation.). The C_{max}, AUC, and T_{max} of rosuvastatin (20 mg single oral dosing) simulated using the modified CL_{int}s of uptake transporters were 25.7±10.1 ng/ml, 235±95.2 ng h/ml, and 3.30 (1.92-3.85) h, respectively (Fig. 2).

Evaluation of the effect of telmisartan on the PK of rosuvastatin using PBPK modeling

Prior to conducting the simulation of drug–drug interaction studies, the $K_{i,BCRP,intestine}$ of telmisartan was estimated. We initially tried $IC_{50,BCRP}$/2 (8.45 μM) using Eq. (1) as the $K_{i,BCRP,intestine}$ of telmisartan. However, the AUC_I/AUC and C_{maxI}/C_{max} of rosuvastatin (with/without telmisartan) predicted thereby were both 1.00-fold which implied that the calculated $K_{i,BCRP,intestine}$ (8.45 μM)

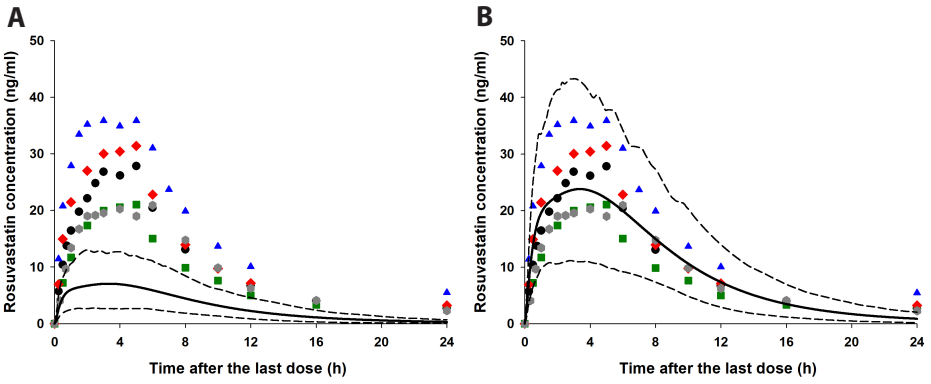

Fig. 2. Simulated and observed plasma concentration–time profile of rosuvastatin after a single oral administration of 20 mg rosuvastatin. Simulated concentration profiles of 10 trials are represented by solid lines (mean) and dashed lines (95th and 5th percentiles). (A) Simcyp library model (based on Caucasian data), (B) our model modified using clinical (Korean) data listed in Table 3. Observed data are from references [3,32].

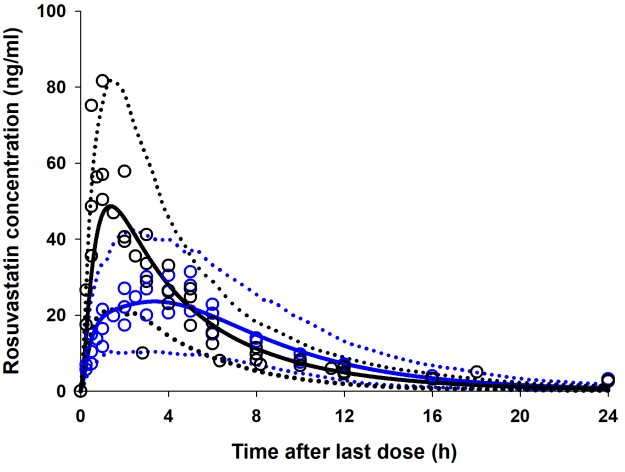

Fig. 3. Simulated and observed plasma concentration–time profiles of rosuvastatin in rosuvastatin–telmisartan study. Plasma concentrations of rosuvastatin (time after the last dose, 0-24 h) were simulated after 20 mg of rosuvastatin was orally coadministered with (black solid line) or without (blue solid line) 80 mg telmisartan for 6 days. The dashed lines represent the upper (95%) and lower (5%) percentile concentrations of rosuvastatin, respectively. Observed data are from references [3,32].

as half the $IC_{50,BCRP}$ (16.9 μM) [13] under-predicted the magnitude of the rosuvastatin–telmisartan interaction. Thus, we carried out SA of $K_{i,BCRP,intestine}$. The $K_{i,BCRP,intestine}$ chosen from SA (0.003 μM) was much lower than 8.45 μM, that obtained from $IC_{50,BCRP}$ and this was used as the as the initial value for the PE module. The final estimate of $K_{i,BCRP,intestine}$ obtained from the PE module (0.005 μM) best explained the observed drug interactions. Thus, this $K_{i,BCRP,intestine}$ value was chosen to be employed in the rosuvastatin–telmisartan interaction study. Assuming that the affinity of BCRP present in the liver and intestine are the same, we also implemented this value to account for the possible inhibition of BCRP transporter existing in hepatocytes.

After the simulation of clinical studies, the predicted changes in plasma concentration–time profiles of rosuvastatin upon coadministration of telmisartan are overlaid with reported data in Fig. 3. The observed and predicted C_{max}, T_{max}, and AUC of 20 mg rosuvastatin with or without coadministration of 80 mg telmisartan are listed in Table 2. The predicted AUC_I/AUC (1.14) and C_{maxI}/C_{max} (1.92) of rosuvastatin were similar to those reported by Son et al. (AUC_I/AUC 1.18 and C_{maxI}/C_{max} 2.01) [3]. The changes in gut and liver rosuvastatin concentrations were predicted to elucidate the intestinal BCRP-mediated interactions. In the GI tract, telmisartan increased the enterocyte concentration of rosuvastatin by 2.20-fold (Fig. 4, the representative intestinal segment, jejunum), that indicated the inhibition of BCRP efflux transporter by telmisartan. Extracellular and intracellular concentrations of rosuvastatin in liver were also available in these models (Fig. 5). Changes in the extracellular and intracellular rosuvastatin concentration-time profiles of rosuvastatin by telmisartan were almost identical (accelerated T_{max} and increased C_{max}), thus the extracellular/intracellular AUC ratio of rosuvastatin did not change at all (0.203 without telmisartan versus 0.201 with telmisartan). Moreover, the change in sinusoidal uptake clearance of rosuvastatin is insignificant. These results also imply that the hepatic transporter-mediated interaction by telmisartan is negligible.

Evaluation of the effect of cyclosporine on the PK of rosuvastatin using PBPK modeling

The simulated whole blood concentration–time profiles of cyclosporine after 200 mg BID oral administration well explained the observed data (Fig. 6B). The predicted changes of plasma exposures of rosuvastatin are shown in Fig. 6A and the PK parameters are listed in Table 2. The changes in gut and liver rosuvastatin concentrations were also estimated in this simulation. The predicted enterocyte concentrations of rosuvastatin in the presence of cyclosporine were 3.27-fold higher than those of rosuvastatin alone. In hepatocytes, the extracellular/intracellular AUC ratio of rosuvastatin was predicted to increase by 22.7% by cyclosporine (0.203 without cyclosporine versus 0.249 with cyclosporine) and this implied that both of BCRP and OATP1B1/3-mediated interactions by cyclosporine play an important role in rosuvastatin disposition. The change in sinusoidal uptake clearance of rosuvastatin by cyclosporine appeared significant compared to that by telmisartan (Fig. 5B).

DISCUSSION

This study primarily aimed to demonstrate that the BCRP-mediated drug interactions are critical in rosuvastatin by presenting two example cases. The first case is the rosuvastatin–telmisartan study. The primacy of the contribution of the intestinal BCRP transporter seems to be in accord with the PK characteristics of telmisartan and rosuvastatin. Telmisartan (T_{max} 0.75 h) is absorbed faster than rosuvastatin (T_{max} 5 h), presumably due to its highly permeable absorption in the GI tract. The Simcyp-predicted intestinal tissue concentration of telmisartan multiplied by $f_{u,gut}$ (0.015) increased above its $K_{i,BCRP,\ intestine}$ (0.005 μM) immediately after administration, and was maintained for about 9 h (data not shown). In other words, Simcyp predicted that telmisartan pre-occupied the binding sites of intestinal BCRP owing to its faster absorption characteristic, before rosuvastatin molecules could engage with the BCRP transporters, resulting in its accelerated absorption (C_{max}↑, T_{max}↓) without evident decrease in systemic clearance. Mixed-effects modeling results also supported that the rosuvastatin population PK parameter changes by telmisartan implied a modest increase (1.3-fold) in relative bioavailability despite the drastic acceleration of the absorption rate [32].

The second case is the rosuvastatin–cyclosporine study which supports the view that both of the BCRP and OATP1B1/3 transporters contribute to the increased exposure of rosuvastatin. Unlike the rosuvastatin–telmisartan case, hepatic OATP1B1/3-mediated interactions were crucial because cyclosporine exhibited more potent inhibitory effects ($K_{i,\ OATP1B1}$=0.014 μM, $K_{i,\ OATP1B3}$=0.007 μM) against OATP1B1/3 than telmisartan did ($K_{i,\ OATP1B1}$=0.436 μM, $K_{i,\ OATP1B3}$=1.03 μM). This enabled cyclosporine to reach concentrations sufficient to inhibit OATP1B1/3 at the target site. Reproduced cyclosporine PBPK model well explained the observed data and the simulation results were also accordant

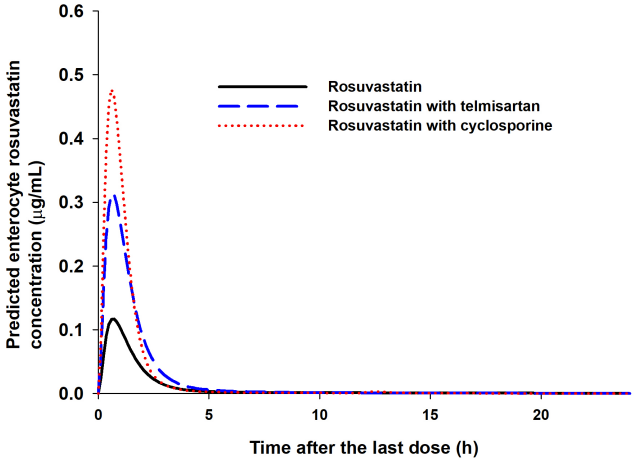

Fig. 4. Predicted enterocyte concentration of rosuvastatin in the jejunum I, a representative GI segment.

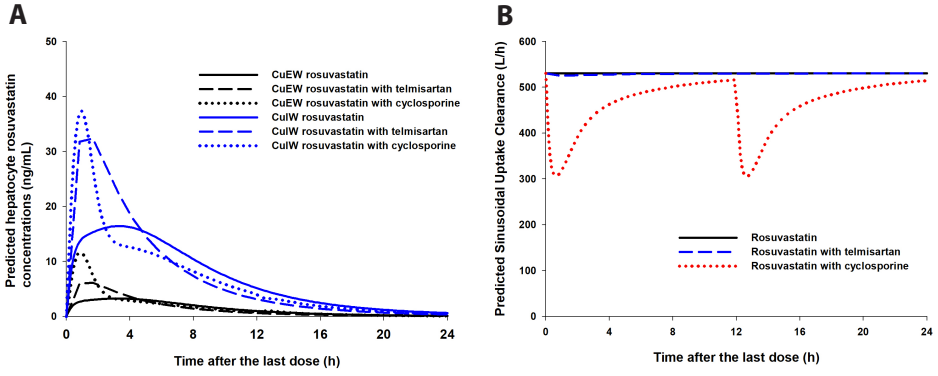

Fig. 5. Predicted hepatic unbound extracellular water concentration (Cu_{EW}, lower black lines) and hepatic unbound intracellular water concentration (Cu_{IW}, upper blue lines) of rosuvastatin (A) and sinusoidal uptake clearance of rosuvastatin (B).

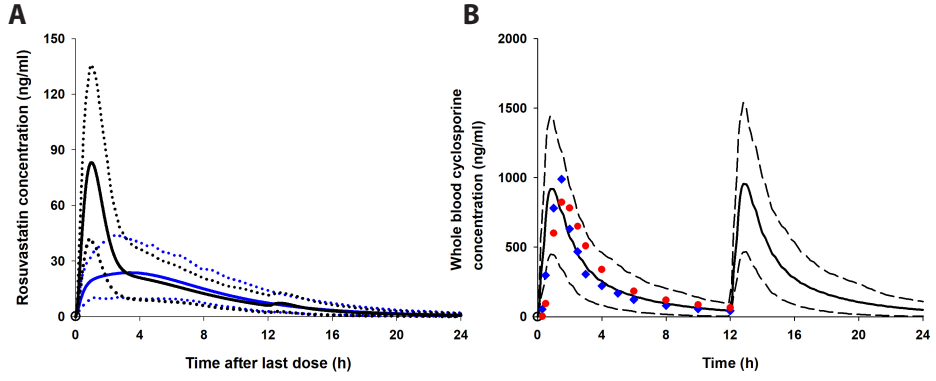

Fig. 6. Simulated plasma concentration–time profiles of rosuvastatin in rosuvastatin–cyclosporine study (A) and simulated *vs.* observed whole blood exposures of cyclosporine (B). The dashed lines represent the upper (95%) and lower (5%) percentile concentrations of rosuvastatin (A) and cyclosporine (B). Dots are observed data from references [34,35].

with those in Jamei's report [4].

The changes in gut and liver rosuvastatin concentration profiles were also predicted in our study. Using the Advanced Dissolution, Absorption and Metabolism (ADAM) model implemented in Simcyp, changes in rosuvastatin concentration in each segment were predicted. In the representative intestinal segment (jejunum), one of the segments where the BCRP transporters are abundantly expressed [41], the rosuvastatin exposure in enterocytes was 2.20-fold and 3.27-fold higher in the presence of telmisartan and cyclosporine, respectively (Fig. 4, patterns in the other segments were similar: data not shown), supporting the hypothesis that the BCRP transporter is a major cause of drug interactions of rosuvastatin in both cases.

Increased absorption of rosuvastatin by telmisartan and cyclosporine has driven a greater fraction of rosuvastatin to reach the liver and caused accelerated T_{max} and increased C_{max} in both extracellular water and intracellular water of hepatocytes. However, there are critical differences in two cases. In the case of telmisartan interactions, it is of note is that the hepatic uptake of rosuvastatin was increased by telmisartan without a change in extracellular water/intracellular water rosuvastatin AUCs, despite its known inhibition of OATP1B1/1B3 transporters ($K_{i,OATP1B1/OATP1B3,\ hepatic}$ values of 0.436 and 1.03 μM, respectively) [10,11]. On the contrary, in the case of cyclosporine interactions, extracellular/intracellular rosuvastatin AUC ratios in hepatocytes increased by 22.7% in the presence of cyclosporine, which indicated that rosuvastatin uptake into the hepatocyte was reduced. Similarly, predicted sinusoidal uptake clearance of rosuvastatin did not change in the presence of telmisartan whereas that of rosuvastatin was reduced in the presence of cyclosporine (Fig. 5B).

There is another report supporting this inference. Gemfibrozil inhibits OATP1B1-, OATP2B1-, and NTCP-mediated rosuvastatin uptake [20]. In a gemfibrozil–rosuvastatin interaction study in humans, the AUC and C_{max} of rosuvastatin were doubled, whereas those of the metabolite, *N*-desmethyl rosuvastatin, were halved [42]. This implies that gemfibrozil inhibited rosuvastatin uptake into hepatocytes, resulting in the decreased *N*-desmethylation of rosuvastatin by CYP2C9 in hepatocytes. On the other hand, the AUC and C_{max} of *N*-desmethyl rosuvastatin increased by 1.07- and 1.53- fold, respectively, with coadministration of telmisartan in Son's report [3], which was the opposite of the results of the gemfibrozil-rosuvastatin study. Thus, the mechanistic explanation of the interaction between rosuvastatin and telmisartan proposed in this report is: telmisartan inhibits rosuvastatin efflux in the GI tract → the amount of rosuvastatin absorbed into the portal vein is increased → the hepatic uptake of rosuvastatin is increased.

To determine the $K_{i,BCRP,intestine}$ value of telmisartan, we employed a top-down approach using data from five different clinical DDI studies. It is known that some discrepancy exists between *in vitro* and *in vivo* K_i values as exemplified by Kato et al. [43]. Because the *in vitro* $K_{i,BCRP,intestine}$ value under-predicted the effect of telmisartan on the rosuvastatin exposures observed in clinical trials, we decided to use a top-down approach. Hu and his colleagues performed an *in vitro* transporter interaction study with telmisartan and rosuvastatin [25]. Their result was that the efflux ratio of rosuvastatin significantly decreased by 42% by 1 μM of telmisartan and this was consistent with our results.

We used *in vivo* CL_{po} rather than metabolic clearance in hepatocytes ($CL_{int,\ met}$) for the telmisartan CL in the simulation step for the following reasons: 1) an *in vivo* CL_{po} value (25.2 L/h) was suitable to recover the observed telmisartan PK; 2) the metabolic pathway of telmisartan in hepatocytes did not overlap that of rosuvastatin; and 3) the half-life of telmisartan is over 20 h [9] despite the $CL_{int,met}$ of telmisartan being reported as 395 μl/min/mg microsomal protein [44] or 1,210 μl/min/mg microsomal protein [28] belonging to high extraction ratio drugs. The discrepancy between $CL_{int,met}$ and *in vivo* CL_{po} can be explained by the enterohepatic circulation of telmisartan-glucuronide after biliary excretion and deconjugation in the intestine [8,28]. Failure to reflect the reabsorbed portion of telmisartan can result in overestimation of $CL_{int,all}$, leading to overestimation of CL_H, and ultimately, of $CL_{in\ vivo}$. Because there is no quantitative information on biliary-excreted and recirculated telmisartan and its glucuronide, our model did not address the enterohepatic recirculation of telmisartan.

To reproduce rosuvastatin exposure in healthy Korean subjects, the CL_{int} values of uptake transporters were modified. In Asian subjects, the exposure of rosuvastatin is known to be almost twice that in Caucasians [27]. This has been suggested to be due to a race-related difference in CL_H, but not in CL_R or F_aF_g [45]. OATP1B1 (*SLCO1B1*) has single-nucleotide polymorphisms (SNPs) of T521>C (Val174Ala) and A388>G (Asn130Asp) associated with the OATP1B1 **1a* (174Val and 130Asn), **1b* (174Val and 130Asp), **5* (174Ala and 130Asn), and **15* (174Ala and 130Asp) alleles [46], which cause genetic variability in rosuvastatin PK. However, it does not explain the race-related variability of rosuvastatin PK. The allelic frequency of 521T<C, which is closely correlated with rosuvastatin PK, is similar between Asians and Caucasians [21,47]. Despite the *SLCO1B1* genotype being identical between Caucasians and Chinese, the C_{max} and AUC of Chinese were approximately twice those of Caucasians [21,40]. Based on these reports, Tomita et al. [45] suggested that there may be a difference in protein expression levels of hepatic OATP1B1 between Asians and Caucasians. The effect of the genetic polymorphism of OATP1B3 and NTCP on the racial differences in rosuvastatin PK is unclear. Similar to the case of rosuvastatin, pravastatin, another substrate of OATP1B1, showed higher exposure in Asians as well. Li et al. tried to explain this with the OATP1B1 genetic variant, however, more supporting evidences are needed to apply their assertion for PBPK models [48].

A few reports [40,49,50] suggested that the genetic polymorphism of BCRP may have caused inter-racial difference in rosuvastatin exposure, but more studies are needed to conclude this.

Considering the degree of uncertainty with respect to uptake transporter-mediated racial differences, CL_{int} values of hepatic uptake transporters had to be adjusted based on the observed rosuvastatin systemic exposures, which is a limitation of our model. Therefore, quantitative prediction of drug interaction potential for telmisartan as an intestinal BCRP inhibitor in this report may be reproduced in other races if appropriate clinical and/or *in vitro* data are available.

In conclusion, our PBPK modeling to evaluate rosuvastatin–telmisartan/cyclosporine interaction revealed that the intestinal BCRP transporter is a major contributor to the interactions.

ACKNOWLEDGMENTS

This study was supported by Basic Science Research Program through the National Research Foundation of Korea (NRF) funded by the Ministry of Science, ICT & Future Planning (NRF-2015R1C1A2A01054495).

CONFLICTS OF INTEREST

The authors declare no conflicts of interest.

REFERENCES

1. Rosamond W, Flegal K, Furie K, Go A, Greenlund K, Haase N, Hailpern SM, Ho M, Howard V, Kissela B, Kittner S, Lloyd-Jones D, McDermott M, Meigs J, Moy C, Nichol G, O'Donnell C, Roger V, Sorlie P, Steinberger J, Thom T, Wilson M, Hong Y; American Heart Association Statistics Committee and Stroke Statistics Subcommittee. Heart disease and stroke statistics--2008 update: a report from the American Heart Association Statistics Committee and Stroke Statistics Subcommittee. *Circulation.* 2008;117:e25-146.
2. Johnson ML, Pietz K, Battleman DS, Beyth RJ. Prevalence of comorbid hypertension and dyslipidemia and associated cardiovascular disease. *Am J Manag Care.* 2004;10:926-932.
3. Son M, Kim Y, Lee D, Roh H, Son H, Guk J, Jang SB, Nam SY, Park K. Pharmacokinetic interaction between rosuvastatin and telmisartan in healthy Korean male volunteers: a randomized, open-label, two-period, crossover, multiple-dose study. *Clin Ther.* 2014;36:1147-1158.
4. Jamei M, Bajot F, Neuhoff S, Barter Z, Yang J, Rostami-Hodjegan A, Rowland-Yeo K. A mechanistic framework for in vitro-in vivo extrapolation of liver membrane transporters: prediction of drug-drug interaction between rosuvastatin and cyclosporine. *Clin Pharmacokinet.* 2014;53:73-87.
5. Simonson SG, Raza A, Martin PD, Mitchell PD, Jarcho JA, Brown CD, Windass AS, Schneck DW. Rosuvastatin pharmacokinetics in heart transplant recipients administered an antirejection regimen including cyclosporine. *Clin Pharmacol Ther.* 2004;76:167-177.
6. Oliverio MI, Coffman TM. Angiotensin-II-receptors: new targets for antihypertensive therapy. *Clin Cardiol.* 1997;20:3-6.
7. Ishiguro N, Maeda K, Kishimoto W, Saito A, Harada A, Ebner T, Roth W, Igarashi T, Sugiyama Y. Predominant contribution of OATP1B3 to the hepatic uptake of telmisartan, an angiotensin II receptor antagonist, in humans. *Drug Metab Dispos.* 2006;34:1109-1115.
8. Ieiri I, Nishimura C, Maeda K, Sasaki T, Kimura M, Chiyoda T, Hirota T, Irie S, Shimizu H, Noguchi T, Yoshida K, Sugiyama Y. Pharmacokinetic and pharmacogenomic profiles of telmisartan after the oral microdose and therapeutic dose. *Pharmacogenet Genomics.* 2011;21:495-505.
9. Stangier J, Schmid J, Türck D, Switek H, Verhagen A, Peeters PA, van Marle SP, Tamminga WJ, Sollie FA, Jonkman JH. Absorption, metabolism, and excretion of intravenously and orally administered [14C]telmisartan in healthy volunteers. *J Clin Pharmacol.* 2000;40:1312-1322.
10. Hirano M, Maeda K, Shitara Y, Sugiyama Y. Drug-drug interaction between pitavastatin and various drugs via OATP1B1. *Drug Metab Dispos.* 2006;34:1229-1236.
11. Zhang A, Wang C, Liu Q, Meng Q, Peng J, Sun H, Ma X, Huo X, Liu K. Involvement of organic anion-transporting polypeptides in the hepatic uptake of dioscin in rats and humans. *Drug Metab Dispos.* 2013;41:994-1003.
12. Deppe S, Ripperger A, Weiss J, Ergün S, Benndorf RA. Impact of genetic variability in the ABCG2 gene on ABCG2 expression, function, and interaction with AT1 receptor antagonist telmisartan. *Biochem Biophys Res Commun*. 2014;443:1211-1217.
13. Weiss J, Sauer A, Divac N, Herzog M, Schwedhelm E, Böger RH, Haefeli WE, Benndorf RA. Interaction of angiotensin receptor type 1 blockers with ATP-binding cassette transporters. *Biopharm Drug Dispos.* 2010;31:150-161.
14. Rubba P, Marotta G, Gentile M. Efficacy and safety of rosuvastatin in the management of dyslipidemia. *Vasc Health Risk Manag.* 2009;5:343-352.
15. Martin PD, Mitchell PD, Schneck DW. Pharmacodynamic effects and pharmacokinetics of a new HMG-CoA reductase inhibitor, rosuvastatin, after morning or evening administration in healthy volunteers. *Br J Clin Pharmacol.* 2002;54:472-477.
16. Martin PD, Warwick MJ, Dane AL, Brindley C, Short T. Absolute oral bioavailability of rosuvastatin in healthy white adult male volunteers. *Clin Ther.* 2003;25:2553-2563.
17. White CM. A review of the pharmacologic and pharmacokinetic aspects of rosuvastatin. *J Clin Pharmacol.* 2002;42:963-970.
18. Bergman E, Forsell P, Tevell A, Persson EM, Hedeland M, Bondesson U, Knutson L, Lennernäs H. Biliary secretion of rosuvastatin and bile acids in humans during the absorption phase. *Eur J Pharm Sci.* 2006;29:205-214.
19. Kitamura S, Maeda K, Wang Y, Sugiyama Y. Involvement of multiple transporters in the hepatobiliary transport of rosuvastatin. *Drug Metab Dispos.* 2008;36:2014-2023.
20. Ho RH, Tirona RG, Leake BF, Glaeser H, Lee W, Lemke CJ, Wang Y, Kim RB. Drug and bile acid transporters in rosuvastatin hepatic uptake: function, expression, and pharmacogenetics. *Gastroenterology.* 2006;130:1793-1806.
21. Lee E, Ryan S, Birmingham B, Zalikowski J, March R, Ambrose H, Moore R, Lee C, Chen Y, Schneck D. Rosuvastatin pharmacokinetics and pharmacogenetics in white and Asian subjects residing in the same environment. *Clin Pharmacol Ther.* 2005;78:330-341.

22. Hu M, To KK, Mak VW, Tomlinson B. The ABCG2 transporter and its relations with the pharmacokinetics, drug interaction and lipid-lowering effects of statins. *Expert Opin Drug Metab Toxicol.* 2011;7:49-62.
23. Ieiri I, Higuchi S, Sugiyama Y. Genetic polymorphisms of uptake (OATP1B1, 1B3) and efflux (MRP2, BCRP) transporters: implications for inter-individual differences in the pharmacokinetics and pharmacodynamics of statins and other clinically relevant drugs. *Expert Opin Drug Metab Toxicol*. 2009;5:703-729.
24. Elsby R, Martin P, Surry D, Sharma P, Fenner K. Solitary inhibition of the breast cancer resistance protein efflux transporter results in a clinically significant drug-drug interaction with rosuvastatin by causing up to a 2-fold increase in statin exposure. *Drug Metab Dispos.* 2016;44:398-408.
25. Hu M, Lee HK, To KK, Fok BS, Wo SK, Ho CS, Wong CK, Zuo Z, Chan TY, Chan JC, Tomlinson B. Telmisartan increases systemic exposure to rosuvastatin after single and multiple doses, and in vitro studies show telmisartan inhibits ABCG2-mediated transport of rosuvastatin. *Eur J Clin Pharmacol.* 2016;72:1471-1478.
26. Kim KT, Birmingham BK, Azumaya CT, Chen Y, Schneck D, Zalikowski J. Increased systemic exposure to rosuvastatin in Asian subjects residing in the United States compared to Caucasian subjects. *Clin Pharmacol Ther.* 2008;83:S14.
27. US Food and Drug Aministration. Clinical pharmacology and biopharmaceutics review. Rockville, MD.: US Food and Drug Aministration; 2006. Report No.: NDA 21-366 Crestor. 15 p.
28. Li R, Ghosh A, Maurer TS, Kimoto E, Barton HA. Physiologically based pharmacokinetic prediction of telmisartan in human. *Drug Metab Dispos.* 2014;42:1646-1655.
29. Yang J, Jamei M, Yeo KR, Tucker GT, Rostami-Hodjegan A. Prediction of intestinal first-pass drug metabolism. *Curr Drug Metab.* 2007;8:676-684.
30. Rodgers T, Rowland M. Physiologically based pharmacokinetic modelling 2: predicting the tissue distribution of acids, very weak bases, neutrals and zwitterions. *J Pharm Sci.* 2006;95:1238-1257.
31. Son H, Roh H, Lee D, Chang H, Kim J, Yun C, Park K. Pharmacokinetics of rosuvastatin/olmesartan fixed-dose combination: a single-dose, randomized, open-label, 2-period crossover study in healthy Korean subjects. *Clin Ther.* 2013;35:915-922.
32. Park WS, Jang D, Han S, Yim DS. Mixed-effects analysis of increased rosuvastatin absorption by coadministered telmisartan. *Transl Clin Pharmacol*. 2016;24:55-62.
33. Cer RZ, Mudunuri U, Stephens R, Lebeda FJ. IC50-to-Ki: a web-based tool for converting IC50 to Ki values for inhibitors of enzyme activity and ligand binding. *Nucleic Acids Res.* 2009;37:W441-445.
34. Lim MS, Seong SJ, Park J, Seo JJ, Lee J, Yu KS, Lee HW, Yoon YR. Assessment of pharmacokinetic proportionality of levofloxacin and cyclosporine over a 100-fold dose range in healthy human volunteers. *Expert Opin Drug Metab Toxicol.* 2012;8:399-405.
35. Oliveira-Freitas VL, Dalla Costa T, Manfro RC, Cruz LB, Schwartsmann G. Influence of purple grape juice in cyclosporine bioavailability. *J Ren Nutr.* 2010;20:309-313.
36. Yamada A, Maeda K, Ishiguro N, Tsuda Y, Igarashi T, Ebner T, Roth W, Ikushiro S, Sugiyama Y. The impact of pharmacogenetics of metabolic enzymes and transporters on the pharmacokinetics of telmisartan in healthy volunteers. *Pharmacogenet Genomics.* 2011;21:523-530.
37. Zhang P, Zhang Y, Chen X, Li R, Yin J, Zhong D. Pharmacokinetics of telmisartan in healthy Chinese subjects after oral administration of two dosage levels. *Arzneimittelforschung.* 2006;56:569-573.
38. Stangier J, Su CA, Roth W. Pharmacokinetics of orally and intravenously administered telmisartan in healthy young and elderly volunteers and in hypertensive patients. *J Int Med Res.* 2000;28:149-167.
39. Noh YH, Lim HS, Kim MJ, Kim YH, Choi HY, Sung HR, Jin SJ, Lim J, Bae KS. Pharmacokinetic interaction of telmisartan with s-amlodipine: an open-label, two-period crossover study in healthy Korean male volunteers. *Clin Ther.* 2012;34:1625-1635.
40. Birmingham BK, Bujac SR, Elsby R, Azumaya CT, Zalikowski J, Chen Y, Kim K, Ambrose HJ. Rosuvastatin pharmacokinetics and pharmacogenetics in Caucasian and Asian subjects residing in the United States. *Eur J Clin Pharmacol.* 2015;71:329-340.
41. Harwood MD, Achour B, Neuhoff S, Russell MR, Carlson G, Warhurst G, Rostami-Hodjegan A. In vitro-in vivo extrapolation scaling factors for intestinal P-glycoprotein and breast cancer resistance protein: part II. The impact of cross-laboratory variations of intestinal transporter relative expression factors on predicted drug disposition. *Drug Metab Dispos.* 2016;44:476-480.
42. Schneck DW, Birmingham BK, Zalikowski JA, Mitchell PD, Wang Y, Martin PD, Lasseter KC, Brown CD, Windass AS, Raza A. The effect of gemfibrozil on the pharmacokinetics of rosuvastatin. *Clin Pharmacol Ther.* 2004;75:455-463.
43. Pang KS, Rodrigues AD, Peter RM. Enzyme- and transporter-based drugd-drug interactions. New York: Springer; 2010. p.301-307.
44. Gill KL, Houston JB, Galetin A. Characterization of in vitro glucuronidation clearance of a range of drugs in human kidney microsomes: comparison with liver and intestinal glucuronidation and impact of albumin. *Drug Metab Dispos.* 2012;40:825-835.
45. Tomita Y, Maeda K, Sugiyama Y. Ethnic variability in the plasma exposures of OATP1B1 substrates such as HMG-CoA reductase inhibitors: a kinetic consideration of its mechanism. *Clin Pharmacol Ther.* 2013;94:37-51.
46. Trdan Lušin T, Stieger B, Marc J, Mrhar A, Trontelj J, Zavratnik A, Ostanek B. Organic anion transporting polypeptides OATP1B1 and OATP1B3 and their genetic variants influence the pharmacokinetics and pharmacodynamics of raloxifene. *J Transl Med.* 2012;10:76.
47. Niemi M, Pasanen MK, Neuvonen PJ. Organic anion transporting polypeptide 1B1: a genetically polymorphic transporter of major importance for hepatic drug uptake. *Pharmacol Rev.* 2011;63:157-181.
48. Li R, Barton HA, Maurer TS. Toward prospective prediction of pharmacokinetics in OATP1B1 genetic variant populations. *CPT Pharmacometrics Syst Pharmacol.* 2014;3:e151.
49. Elsby R, Hilgendorf C, Fenner K. Understanding the critical disposition pathways of statins to assess drug-drug interaction risk during drug development: it's not just about OATP1B1. *Clin Pharmacol Ther.* 2012;92:584-598.
50. Sakiyama M, Matsuo H, Takada Y, Nakamura T, Nakayama A, Takada T, Kitajiri S, Wakai K, Suzuki H, Shinomiya N. Ethnic differences in ATP-binding cassette transporter, sub-family G, member 2 (ABCG2/BCRP): genotype combinations and estimated functions. *Drug Metab Pharmacokinet.* 2014;29:490-492.